International Journal on Magnetic Particle Imaging
Vol 9, No 1, Suppl 1, Article ID 2303028, 3 Pages

Infinite Science Publishing

Proceedings Article

2D Projection Imaging with a Single-Sided FFL Magnetic Particle Imaging Scanner

Chris McDonough [a] · Alexey Tonyushkin [a,*]

[a] Physics Department, Oakland University, Rochester, MI 48309 USA
[*] Corresponding author, email: tonyushkin@oakland.edu

Abstract

There have been several MPI scanner designs with the promise of useful clinical imaging. One such promising design is the so called single-sided scanner, which limits all hardware to a single side of the device. This provides the scanner with an unrestricted imaging volume, but at the cost of finite imaging depth and inhomogeneous magnetic fields. Our group has designed such a scanner that utilizes an FFL for spatial encoding, which differs from the original single-sided scanner which utilizes an FFP. In this work we demonstrate the first two dimensional images obtained using a single-sided FFL MPI scanner.

I. Introduction

Typical Magnetic Particle Imaging (MPI) scanner makes use of a closed bore topology [1], however there are significant efforts required for this topology to scale up to full body imaging due to high-power requirements. Therefore an alternative scanner topology capable of obtaining clinically useful images is desired. One promising design is the single-sided scanner topology, which restricts all hardware to a single side of the device [2].

Our group has designed a single-sided scanner that utilizes a field free line (FFL) [3, 4], which differs from the original single-sided scanner that utilizes a field free point (FFP) [5, 6]. FFL offers a number of benefits when compared to FFP including higher sensitivity, and access to robust reconstruction techniques first developed for computed tomography [7]. In this work we present the first 2D imaging of various phantoms as a proof of principle of our design.

II. Methods and materials

II.I. Single-Sided Scanner

Our single-sided scanner (see Fig. 1(a)) consists of five electromagnetic coils, three of which are "race-track" shaped and are embedded inside a water cooled enclosure [4]. Two of the embedded coils are responsible for creating the FFL and used for spatial encoding. Applying equal DC currents to these selection coils creates an FFL 17 mm above the surface of the scanner along the long axis of our scanner. Modulating the relative current between the two selection coils changes the position of the FFL, which allows for scanning the FFL across the subject. The third embedded coil located below the selection coils in the center of the scanner is responsible for exciting the superparamagnetic iron oxide (SPIO) sample.

Two circular coils located at the surface of the scanner are used as the receive coils in a surface gradiometer arrangement [8]. One of them is the primary detection coil and the other identical one is the compensation coil. Using the gradiometer receive coils allows for attenuation of the background signal without use of an additional receive filter.

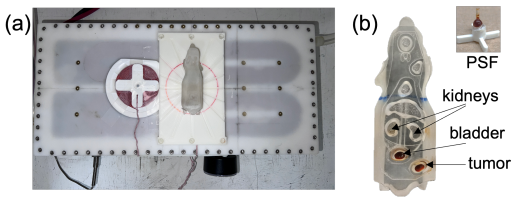

Figure 1: a) Top view of the single-sided FFL scanner with a subject's stand on top of the receive coil and a mouse phantom; b) an anatomical mouse phantom with various organs and a PSF small-volume phantom.

II.II. Phantoms

As a prerequisite to *in-vivo* imaging we used a single and double rod in orthogonal orientation, i.e., "elbow" mimicking blood vessels as well as an anatomical mouse phantom (see Fig. 1(b)). Each rod has a diameter of 1.2 mm and a length of 10 mm and filled with undiluted Synomag-D SPIO. In a mouse phantom imaging, an anatomical 3D printed fillable mouse phantom (BIOEMTECH) was used. Two different regions of interest were imaged. In the first experiment kidneys were filled with 300 μl each of undiluted SPIO Vivotrax+ (MagneticInsight). In the second experiment a bladder with a volume of 294 μl and a "tumor" site with a volume of 204 μl were both filled with an undiluted SPIO Synomag-D (Micromod). Each phantom has protrusions located on the bottom, which are designed to fit into grooves located on the rotational table. These grooves allow for precise manual rotations of the phantom.

II.III. Imaging

To excite the SPIO in our samples we applied an oscillating magnetic field at 25 kHz at the surface of the scanner generated by a drive coil. The phantom was placed on a subject table with the graduated angles corresponding to 8 rotation steps imaged from 0° to 180° with 4 cm x 4 cm FOV in the horizontal cross-section at the penetration depth of 17 mm. For each angle position the signal was obtained with the FFL moving from -2 cm to 2 cm with a step of 1 mm and the background was subtracted from the average. A sinogram was collected and back-projected to obtain a 2D image. To further reduce noise in the final images averaging of the projections in the sinogram was preformed for certain phantoms. This was done for the "elbow" phantom and the mouse bladder plus tumor phantom. The averaging was done by obtaining on average 36 projections at each angle before manual rotation of the subject. A separate PSF image was experimentally obtained with the symmetrical point source of a glass bulb (see Fig. 1 (b)) placed at the center and containing 18 μl of SPIO. A deconvoluted image was overlaid with to-scale picture of the mouse phantom to obtain the contour lines of the mouse and various organs.

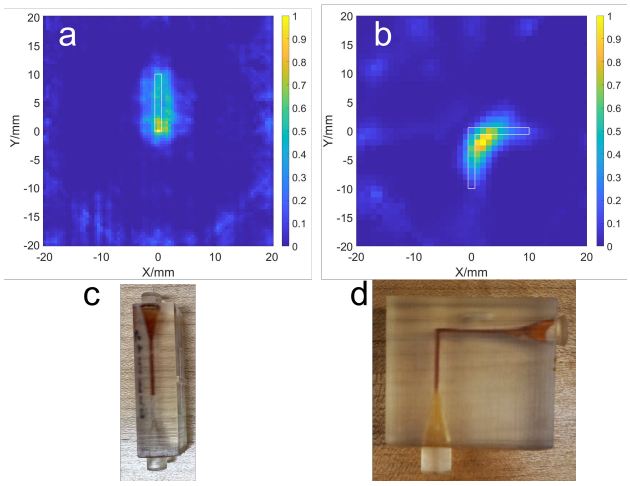

Figure 2: Reconstructed images of a single rod (a) and elbow rod (b) phantoms and the corresponding 3D printed phantoms: (c) single rod, (d) elbow rods. Here, G = 0.58 T/m, B_{drive} =1.6 mT, SPIO: Synomag-D.

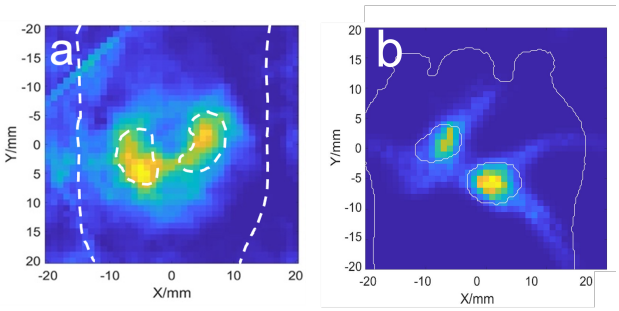

Figure 3: Horizontal cross-section slices of back-projection reconstructed imaging over FOV = 4 x 4 cm^2 of various organs of a mouse phantom. a) Kidneys filled with Vivotrax+, excited with B_{drive} = 1.6 mT; b) bladder and "tumor" site filled with an undiluted Synomag-D, excited with B_{drive} = 1.2 mT. The dashed and solid white lines correspond to overlays of the mouse phantom and organs. Here, G = 0.58 T/m.

III. Results and Discussion

To demonstrate the two dimensional imaging capability of our single-sided MPI scanner we imaged multiple phantoms. There were two types of phantoms imaged in this study, the first being the rod type phantoms, which mimic blood capillaries. The second is an anatomical mouse phantom (see Fig. 1(b)), which has irregular volumes designed to mimic the size and shape of typical mouse organs.

Imaging of the single rod phantom is shown in Fig. 2(a). From this image the structure of the phantom is visible, demonstrating that our scanner is capable of imaging straight capillary objects. Under these conditions we are also able to image bent capillary objects, as is demonstrated in Fig. 2(b). Our scanner is also able

10.18416/ijmpi.2023.2303028

to distinguish irregular volumes separated by 4 mm, as seen in Fig. 3(a,b). Some artifacts streaking artifacts can be seen in the mouse organ phantom, these artifacts are likely attributed to low angular resolution and will be alleviated in the future.

The noise reduction was performed for the "elbow" phantom (see Fig. 2(b,d)), and the mouse bladder plus tumor phantom (see Fig. 3(b)). For comparison, imaging of a rod (Fig. 2(a,c))) and kidneys (Fig. 3(a)) did not include averaging of projections that resulted in noisy images.

In the future experiments we will improve angular resolution through the introduction of a custom made, stepper motor controlled, rotation table. This rotational table will allow us to automatically rotate the subject with an angular resolution of 1.8°. Another potential improvement is to increase the maximum magnetic field field gradient achievable by our scanner. This can be done through the introduction of higher power supplies, which are capable of delivering a higher current to the selection coils.

IV. Conclusion

We have demonstrated the first experimental two dimensional images obtained using a single-sided FFL MPI scanner. These images demonstrate the viability of our scanner for imaging capillaries and irregular volumes, such as the organs of a mouse. Additionally, these results were obtained with a limited angular resolution 22.5°, and with low gradient ~ 0.6 T/m. In the future we aim to improve 2D imaging by using higher angular and spatial resolutions.

Acknowledgments

Research funding: this work is supported by NIH under Award R15EB028535.

Author's statement

Conflict of interest: Authors state no conflict of interest.

References

[1] B. Gleich and J. Weizenecker. Tomographic imaging using the nonlinear response of magnetic particles. *Nature*, 435(7046):1214–1217, 2005, doi:10.1038/nature03808.

[2] T. F. Sattel, T. Knopp, S. Biederer, B. Gleich, J. Weizenecker, J. Borgert, and T. M. Buzug. Single-sided device for magnetic particle imaging. *Journal of Physics D: Applied Physics*, 42(2):022001, 2009, doi:10.1088/0022-3727/42/2/022001.

[3] A. Tonyushkin. Single-Sided Field-Free Line Generator Magnet for Multi-Dimensional Magnetic Particle Imaging. *IEEE Transactions on Magnetics*, 53(9):5300506, 2017, doi:10.1109/TMAG.2017.2718485.

[4] J. Pagan, C. McDonough, T. Vo, and A. Tonyushkin. Single-sided magnetic particle imaging device with field-free-line geometry for in vivo imaging applications. *IEEE Transactions on Magnetics*, 57(2):5300105, 2021, doi:10.1109/TMAG.2020.3008596.

[5] K. Gräfe, A. von Gladiss, G. Bringout, M. Ahlborg, and T. M. Buzug. 2D Images Recorded With a Single-Sided Magnetic Particle Imaging Scanner. *IEEE Transactions on Medical Imaging*, 35(4):1056–1065, 2016, doi:10.1109/TMI.2015.2507187.

[6] A. von Gladiss, Y. Blancke Soares, T. M. Buzug, and K. Gräfe, Dynamic imaging with a 3d single-sided mpi scanner, in *International Workshop on Magnetic Particle Imaging*, 235–236, 2019.

[7] J. Weizenecker, B. Gleich, and J. Borgert. Magnetic particle imaging using a field free line. *Journal of Physics D: Applied Physics*, 41(10):105009, 2008, doi:10.1088/0022-3727/41/10/105009.

[8] C. McDonough, J. Pagan, and A. Tonyushkin. Implementation of the surface gradiometer receive coils for the improved detection limit and sensitivity in the single-sided mpi scanner. *Physics in Medicine & Biology*, 2022, doi:10.1088/1361-6560/aca5ec.